Available online at www.sciencedirect.com
SCIENCE DIRECT®
Journal of Catalysis 221 (2004) 466–473
JOURNAL OF CATALYSIS
www.elsevier.com/locate/jcat

Segregation of platinum from mordenite channels on calcination and reduction pretreatments

Shanmugam Yuvaraj,[a] Tsong-Huei Chang,[b] and Chuin-Tih Yeh [a,*]

[a] *Department of Chemistry, National Tsing Hua University, Hsinchu 30043, Taiwan, Republic of China*
[b] *Department of Chemistry, Ming Hsing University of Science and Technology, Hsinchu 30043, Taiwan, Republic of China*

Received 25 June 2003; revised 29 August 2003; accepted 5 September 2003

Abstract

Samples of Pt/NaMOR (Pt/NaM) and Pt/HMOR (Pt/HM) were prepared through ion exchange of MOR with $[Pt(NH_3)_4](NO_3)_2$ and subsequently treated with calcination at 723 K in air and reduction at 673 K in H_2. The segregation of Pt in the prepared samples during the treatment was monitored with different characterization techniques. Transmission electron microscopy results showed that platinum in freshly exchanged and in calcined samples stayed dominantly in channels of MOR. However, a significant portion of platinum in channels segregated to and sintered at the external surface during the reduction. A high N_H/N_{Pt} ratio of 0.80 in 0.5Pt/NaM compared to that of 0.55 in 0.5Pt/HM in hydrogen chemisorption suggested that the segregation of platinum was partially retarded by Na^+ ions in NaM. Xenon tended to physisorb on reduced Pt particles in the channels of Pt/NaM and caused a downfield shift to ^{129}Xe NMR peak. The shift revealed that a fraction of segregated platinum (or a fraction of Pt retained in the channels) remained constant for Pt/NaM samples with different Pt loadings. Pt particles retained in channels of highly loaded 5Pt/NaM blocked pores ($d \sim 0.70$ nm) and thereby substantially blocked the diffusion of gas molecules. Consequently, a low uptake of both hydrogen and xenon in 5Pt/NaM was observed in isotherm measurements.

Keywords: Mordenite; Platinum segregation; Pore blockage; ^{129}Xe NMR, TPR

1. Introduction

Mordenite (MOR) is a zeolite with 12-membered (0.65 × 0.70 nm) channels. They are in parallel to each other along the z direction and interconnected by 0.48-nm deep 8-membered pockets (Fig. 1). Platinum-dispersed mordenite is a bifunctional catalyst, active for isomerization of n-alkanes and aromatization of paraffins [1,2]. Activity of Pt samples depends on platinum distribution and dispersion, which are often affected by segregation and agglomeration of platinum during pretreatments, viz. calcination and reduction.

Segregation of Pt in zeolites is a phenomenon involving migration of Pt from channels to the external surface. Generally, segregation is assessed from the change in size or location of Pt particles. In the literature, several techniques, including temperature-programmed reduction (TPR), transmission electron microscopy (TEM), hydrogen chemisorption, and X-ray diffraction, have been employed to study the segregation of Pt particles.

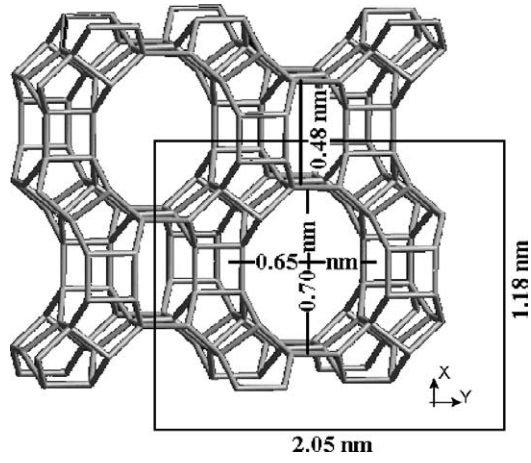

Fig. 1. Lattice structure of MOR showing parallel channels of ∼ 0.7 nm size in z axis and the interconnecting pockets of 0.48 nm in y axis.

* Corresponding author.
E-mail address: ctyeh@mx.nthu.edu.tw (C.-T. Yeh).

0021-9517/$ – see front matter
doi:10.1016/j.jcat.2003.09.008

Table 1
TPR data published in the literature for supported Pt catalysts

Sample	Pt species	T_r (K)	Location	Precursor	Refs.
Pt/Al_2O_3	Pt_eO	323	External	$PtCl_4$	[12,13]
	Pt_eO_2	373			
	Pt-aluminate	493			
Pt/SiO_2	Pt_eO	223	External	$[Pt(NH_3)_4]Cl_2$	[12,13]
	Pt_eO_2	293		$[Pt(NH_3)_4](NO_3)_2$	
Pt/NaY	Pt_cO	373	Super cage	$[Pt(NH_3)_4](NO_3)_2$	[9]
Pt/KL	Pt_eO	298	External	$[Pt(NH_3)_4]Cl_2$	[10,11]
	Pt_cO	353	Channel		
Pt/Naβ	Pt_eO	223	External	$[Pt(NH_3)_4](NO_3)_2$	[8]
	Pt_cO	353	Channel		

TPR has been shown as a versatile technique to identify the environment of platinum in Pt-dispersed samples [3–13]. Since segregation of platinum involves a change of environment, TPR technique can be conveniently used to assess segregation of platinum in MOR samples. Platinum species in different environments are reduced at different temperatures (T_r) in TPR. The T_rs of Pt-oxides in various environments in Pt loaded alumina, silica, and zeolites-Y, L and β have been reported in the literature [3–13] and were summarized in Table 1. The Pt-oxides dispersed on the external surface (Pt_eO) of zeolites are reduced generally at a lower temperature ($T_r < 350$ K) than those ($T_r > 350$ K) in channels (Pt_eO) of zeolites.

In the literature, Pt in zeolite-supported samples has also been studied [14–22] with another environment-sensitive technique, ^{129}Xe nuclear magnetic resonance (^{129}Xe NMR). Table 2 lists the literature on ^{129}Xe NMR of platinum dispersed in KL, NaY, NaEMT, MCM-41, and γ-alumina. Generally, a downfield shift was observed from Pt samples with Pt loading > 2 wt% [17–19]. A higher downfield shift was generally found from platinum particles in large cages ($\sim$1.3 nm of NaY [17,18] and EMT [19]) than in small channels ($\sim$0.7 nm of Naβ [20] and KL [20–22]).

It has been reported that Pt in channels of KL showed a linear increase in δ with its loading in Pt/KL samples [22].

Table 2
Literature-reported chemical shift (δ) values for xenon in pores of various supports and in pores of their hydrogen-reduced Pt samples at 296 K

Sample (wt% Pt)	Pt (wt%)	P_{Xe} (Torr)	δ (ppm) Support	δ (ppm) Pt/zeolite	Refs.
Pt/γ-Al_2O_3	5.2	675	110	220	[14,15]
Pt/MCM-41	2.0	400	80	141	[16]
Pt/NaY	10.0	400	67	169	[17]
Pt/NaY	4.0	400	80	126	[18]
Pt/EMT	11.0	400	74	208	[19]
Pt/Kβ	0.6	218	71	74	[20]
Pt/KL	0.6	218	105	105	[20]
Pt/KL	1.0	370	106	113	[21]
Pt/KL	0.9	400	118	128	[22]
Pt/KL	5.2	400	118	166	[22]
Pt/NaM	0.5	500	138	151	Present work
Pt/NaM	5.0	500	138	162	Present work

To the best of our knowledge, ^{129}Xe NMR has not been used to study the segregation of platinum particles. In this work, ^{129}Xe NMR is proposed as an indirect method for assessing segregation of platinum. Variation in δ of xenon is monitored with respect to Pt density in the channels of Pt/MOR.

2. Experimental

2.1. Preparation of samples

NaMOR (Si/Al = 9.6; 4.0 wt% Na^+ ions and surface area = 340 $m^2\,g^{-1}$) and corresponding HMOR (HM; Si/Al = 10.3 and surface area = 325 $m^2\,g^{-1}$) were obtained from Tosoh Corporation, Japan. Platinum ion-exchanged MOR samples with 0.5 and 5.0 wt% Pt were prepared using $[Pt(NH_3)_4](NO_3)_2$. Typically for 0.5 wt%, 5×10^{-2} g of $[Pt(NH_3)_4](NO_3)_2$ was dissolved in 500 ml water and then 5 g of either NaM or HM was added to the solution, stirred at 353 K for 24 h, filtered, and repeatedly washed with deionized water. The washed samples are then air-oven-dried at 383 K and labeled as fresh samples of F0.5Pt/NaM and F0.5Pt/HM. The fresh samples were heated in air at a rate of 2 K min^{-1} to 723 K and then calcined for 12 h. Table 3 lists the calcined samples with a prefix C. In a similar manner, the freshly prepared 5.0 wt% Pt samples were labeled as F5Pt/NaM and F5Pt/HM. The Pt content of all the prepared samples (Table 3) was confirmed by ICP-AES.

2.2. Hydrogen chemisorption and xenon physisorption

Isotherms of hydrogen chemisorption and xenon physisorption on reduced Pt particles were obtained at 296 K from a classical volumetric apparatus. The calcined samples were ex situ reduced at 673 K in H_2 for an hour at a

Table 3
Physicochemical data for samples used in this study

Sample	Pt (wt%)	Na (%)	Pt particle size, d_{Pt} (nm) XRD	Pt particle size, d_{Pt} (nm) TEM (average)	N_H/N_{Pt}
HM	–	0.02	–	–	–
NaM	–	4.0	–	–	–
C0.5Pt/NaM	0.52	3.6	–	2–3 5[a]	–
R0.5Pt/NaM	0.52	3.6	12	2–3 18[a]	0.80
R2Pt/NaM	1.91	3.1	23	–	–
C5Pt/NaM	4.93	2.4	5	3–5 5[a]	–
R5Pt/NaM	4.93	2.4	31	2–4 30[a]	0.35
C0.5Pt/HM	0.48	0.02	–	–	–
R0.5Pt/HM	0.48	0.02	18	3–5 24[a]	0.55
R5Pt/HM	4.91	0.02	–	–	–

[a] Size of the largest Pt particles found.

heating rate of 2 K min^{-1}. The reduced samples were degassed at 10^{-5} Torr at 773 K for 12 h in a vacuum system. Then, samples were in situ reduced at 673 K with hydrogen, again degassed at 773 K, and then cooled down to 298 K, for both hydrogen chemisorption and xenon physisorption measurements. All the reduced samples were designated with a prefix R in this paper.

2.3. Transmission electron microscopy

About 5×10^{-3} g of reduced Pt/NaM sample was soaked in ethanol, sonicated for 10 min, and then allowed to settle big zeolite particles. A clear supernatant liquid was dropped on a carbon-coated Cu grid and dried under vacuum. A Jeol TEM 400-keV machine was used for taking photos. In addition, the machine is also equipped with in situ electron diffraction (ED) and energy dispersive X-ray (EDX) facilities.

2.4. X-ray diffraction

X-ray diffractograms of the calcined ($T_c \sim 723$ K) and ex situ reduced (at 673 K with a heating rate of 2 K min^{-1}) Pt samples are recorded in a Philips XRD machine with Cu-K_α ($\lambda = 1.5404$ Å) radiation and compared with blank MOR.

2.5. Temperature-programmed reduction

About 5×10^{-3} g of a calcined sample was taken in a U-shaped TPR cell. The platinum species in the sample was then reduced in hydrogen at 673 K with a heating rate of 2 K min^{-1} and subsequently recalcined at 723 K to PtO_x species under O_2/He stream. The recalcined (with a prefix RC in this paper) sample was then cooled under nitrogen gas to 163 K and then N_2 gas was replaced with a reducing gas mixture of 10% H_2/N_2. The TPR spectrum was recorded at a heating rate of 5 K min^{-1} in two steps. First, the temperature range from 173 to 500 K was recorded using a low-temperature routine and the procedure was described elsewhere [12,23].

2.6. ^{129}Xe nuclear magnetic resonance spectroscopy

About 0.5 to 1.0 g of ex situ reduced Pt/MOR sample was placed into a NMR tube with 10 mm in internal diameter. The tube was connected to a vacuum system and degassed at 723 K at 10^{-5} Torr for 24 h. Before xenon loading, samples were again hydrogen reduced in situ at 673 K, degassed, and then cooled down to 296 K. Xenon loading was done at a predetermined pressure using enriched (82%) ^{129}Xe gas. ^{129}Xe NMR has been recorded at 296 K in a Bruker DSX 400 operating at 110.5 MHz with 15-μs pulse and 0.5-s recycle delay. About 25,000 scans were acquired and the spectra were referenced to xenon in bulk gas mixed with 1–2% O_2.

3. Results and discussion

Fig. 2 compares high-resolution TEM pictures from fresh, calcined, and reduced samples of 0.5Pt/NaM, 0.5Pt/HM and 5Pt/NaM. Fig. 2a shows a homogeneously tinted TEM picture of F0.5Pt/NaM. This picture is similar to that of a blank NaM (not shown). However, fresh F5Pt/NaM displays (Fig. 2b) finely distributed Pt complex grains, mainly in subnanometer sizes. These subnanometer-sized precursors should be inside the channels in view of the cation-exchange capacity (1700 μmol Na^+ g^{-1}) of pores in MOR and the loading ($\sim$ 250 μmol Pt^{2+} g^{-1}) of Pt precursor in the sample. The insets in Figs. 2a and b are diffused ED patterns characteristic of amorphous platinum complex particles.

TEM picture of calcined C5Pt/NaM (Fig. 2c) showed a lot of moderate particles, with $d \sim 3$–5 nm, certainly on the external surface. During calcination at 723 K, Pt precursors are decomposed [Eq. (1)] and a minor fraction of Pt^{2+} should have been autoreduced [Eqs. (2) and (3)] by freed ammonia ligands [4,11,24–26]:

$$[Pt(NH_3)_4]^{2+} \rightarrow Pt^{2+} + 4NH_3, \quad (1)$$

$$Pt^{2+} + 2NH_3 + O_2 \rightarrow N_2 + 2H_2O + Pt + 2H^+, \quad (2)$$

$$2Pt^{2+} + 4NH_3 + xO_2 \rightarrow 4NO_x + 4H_2O + 2Pt + 4H^+. \quad (3)$$

A portion of the reduced Pt-particles might be segregated out from channels and then agglomerated on the external surface as moderate particles [27]. The presence of reduced Pt particles is also confirmed by ED of a selected portion shown in the inset of Fig. 2c.

Fig. 2d displays TEM pictures from the reduced R5Pt/NaM. The picture showed large Pt particle clusters ($\sim$ 30 nm) along with many tiny particles typically in a range of 2–4 nm on the external surface of MOR. These particles may be formed during the reduction treatment by hydrogen:

$$PtO_x + xH_2 \rightarrow Pt + xH_2O. \quad (4)$$

A close examination of the large Pt clusters revealed that they are actually aggregates of moderate particles ($d \sim$ 3–5 nm). During reduction, these aggregates might have formed at the pore mouth of the channels because of a severe segregation of Pt particles. The tiny particles scattered on the surface of mordenite might result from reduction of platinum ions at the external surface. The ED of this sample showed ring patterns ($d \sim 0.26$ nm) characteristic for a crystalline platinum (111) phase.

Despite the severe segregation to the external surface, a large fraction of reduced Pt might have retained in the channels and deposited on their wall. Fig. 2e displayed a fringe pattern ($d \sim$ 0.5–0.7 nm) from R5Pt/NaM and is consistent with the channel dimension (0.65×0.7 nm) of mordenite. Similar patterns have also been found from R0.5Pt/NaM in this study (not shown) and also reported on Pt/KL zeolite [27–29]. The fringe pattern has been described in the literature for platinum in channels.

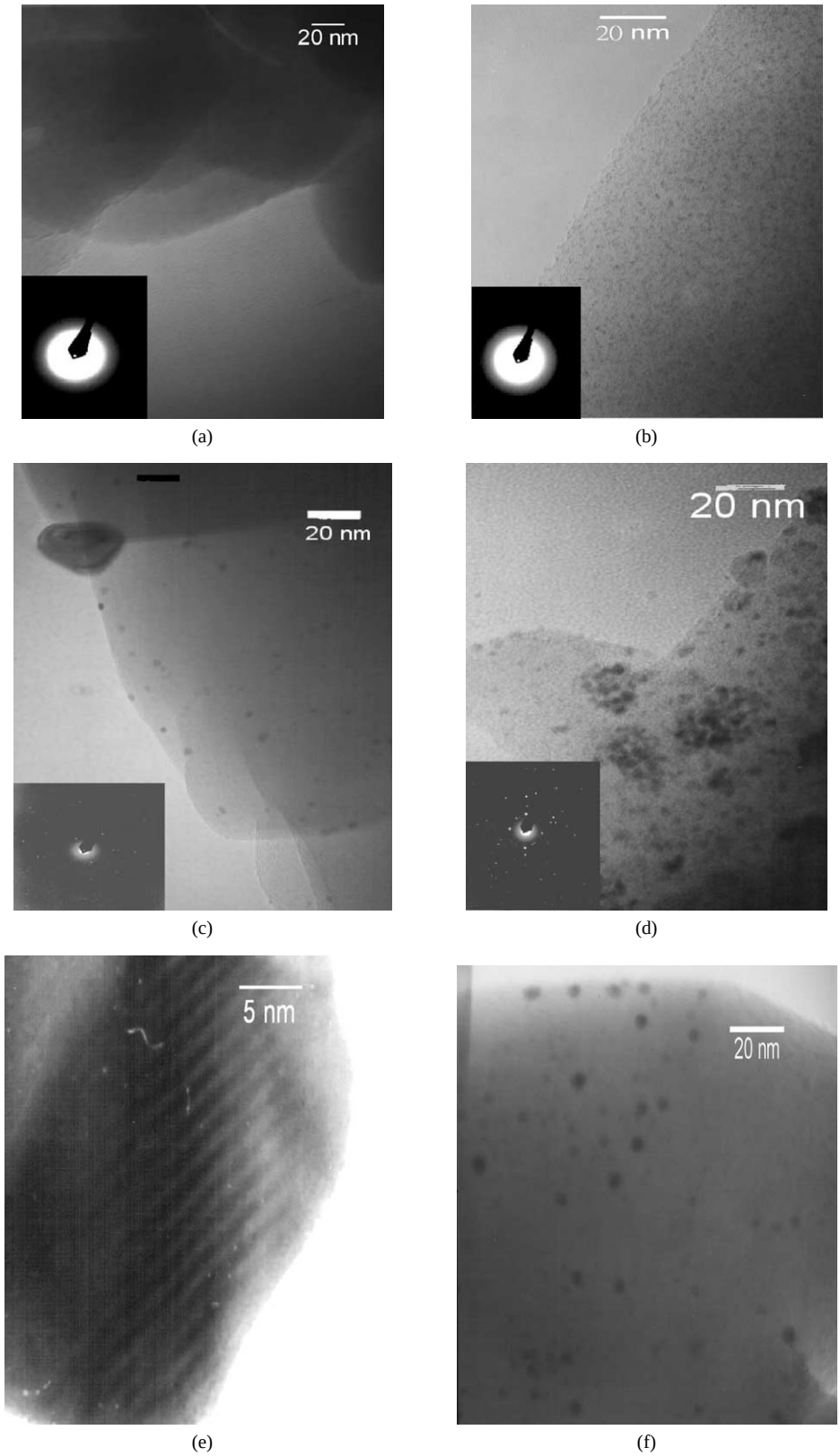

Fig. 2. High-resolution transmission electron micrograms of Pt/NaM samples: (a) F0.5Pt/NaM, (b) F5Pt/NaM, (c) C5Pt/NaM, (d) R5Pt/NaM, (e) fringe pattern from R5Pt/NaM, and (f) R0.5Pt/HM. Insets in 2a–d show electron diffraction pattern of the concerned samples.

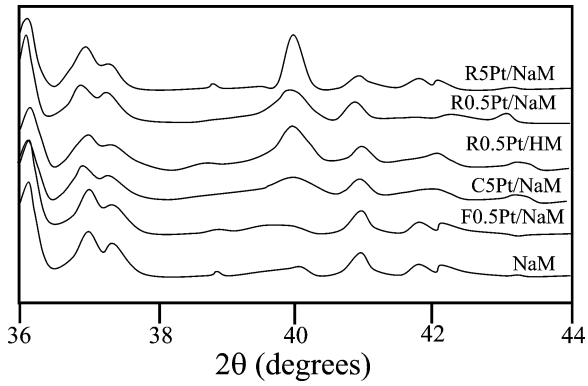

Fig. 3. X-ray diffraction profiles of fresh (F), calcined (C), and reduced (R) samples of Pt/NaM and Pt/HM.

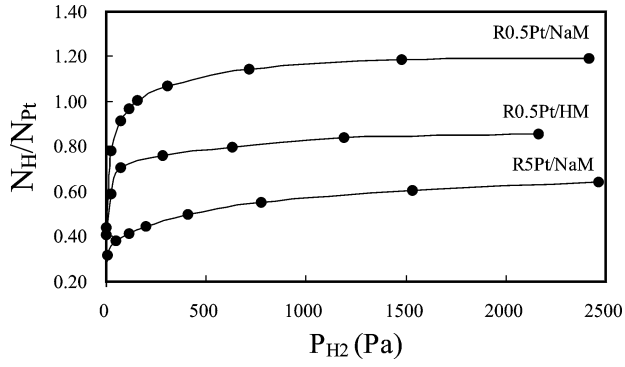

Fig. 4. Hydrogen chemisorption isotherms at 296 K for reduced samples.

Fig. 2f displays TEM picture from the reduced R0.5Pt/HM. The picture showed that the average Pt particles are in a range of 3–5 nm on the external surface of MOR. Surely these particles are larger than those on the R0.5Pt/NaM sample. The ED pattern of the sample well matched with that of R5Pt/NaM. Notably, the fringe pattern is not observed from the R0.5Pt/HM sample and this absence suggested that the abundance of Pt particles is not high enough in the channels of HM. Most of the platinum reduced in the channel of Pt/HM might have segregated out. Obviously, sodium cations in R0.5Pt/NaM sample are more effective in retarding the segregation than protons in R0.5Pt/HM.

Fig. 3 compares the XRD profiles of NaM, F0.5Pt/NaM, C5Pt/NaM, R0.5Pt/NaM, R5Pt/NaM, and R0.5Pt/HM samples. A diffraction peak around $2\theta \sim 40^\circ$ for reduced Pt particles is detected from the calcined and the ex situ-reduced samples but is absent from the fresh sample. The peak from the calcined sample confirmed the prevalence of Pt autoreduction proposed from the TEM results.

Size of large Pt particles ($d_{\mathrm{Pt}} > 5$ nm) formed in the calcined and the reduced samples may be estimated from full width at half-maximum (β) of a broadened Pt peak (111) using Scherrer's equation ($d_{\mathrm{Pt}} = K\lambda/\beta\cos\theta$, where $K = 0.9$) [30]. The estimated sizes are listed in Table 3 along with other physical parameters. The size of Pt particles from R0.5Pt/HM had a larger d_{Pt} (~ 18.0 nm) than that ($d_{\mathrm{Pt}} \sim 12.0$ nm) from R0.5Pt/NaM and also that ($d_{\mathrm{Pt}} \sim 5$–6 nm) from C5Pt/NaM samples. The variation in the calculated d_{Pt} values confirmed that the extent of segregation during pretreatments depends on the cation of the zeolite. Despite of the retardation to segregation by Na^+ ions, a high $d_{\mathrm{Pt}} \sim 31.0$ nm is noted from the highly loaded platinum sample of R5Pt/NaM.

Fig. 4 displays the hydrogen uptake isotherms of three reduced samples—R0.5Pt/NaM, R5Pt/NaM, and R0.5Pt/HM at 298 K. In Fig. 4, it is noted that the chemisorption profile tend to become smooth when $P_{\mathrm{H_2}} > 0.1$ kPa. This indicates that a weak chemisorption may be caused by molecular adsorption of hydrogen [31] on weak sites in the support and also by spillover of hydrogen, especially in the case of alkali-containing zeolites [32,33]. Therefore, a ratio of $N_{\mathrm{H}}/N_{\mathrm{Pt}}$ is obtained between strongly chemisorbed hydrogen (N_{H}) on metal sites, i.e., Pt sites noted in Fig. 4 at $P_{\mathrm{H_2}} \sim 0.1$ kPa [31] and the amount of platinum (N_{Pt}) in a sample.

The obtained $N_{\mathrm{H}}/N_{\mathrm{Pt}}$ values for the reduced Pt samples are listed in the sixth column of Table 3. At a low loading level of 0.5 wt% platinum, the higher ratio obtained from R0.5Pt/NaM ($N_{\mathrm{H}}/N_{\mathrm{Pt}} \sim 0.80$) than that ($N_{\mathrm{H}}/N_{\mathrm{Pt}} \sim 0.55$) from R0.5Pt/HM confirmed the retardation of platinum segregation by sodium ions. But at a level of 5.0 wt% platinum as in R5Pt/NaM, the ratio considerably decreased to ~ 0.35. This is contrary to TEM results that showed a similarity in size (2–4 nm) of the average Pt particles on the external surface of R0.5Pt/NaM and R5Pt/NaM. Therefore, the low $N_{\mathrm{H}}/N_{\mathrm{Pt}}$ ratio for R5Pt/NaM indicated a severe pore blockage, which may prevent the access of platinum in pores by hydrogen molecule ($d_{\mathrm{H_2}} \sim 0.3$ nm). Similar inaccessibility of Pt in the channels of 0.5Pt/KL by CO gas [11] and that of Pt in the sodalite cages of 5.8Pt/NaY [34] has been reported in the literature.

The distribution of platinum in reduced samples has been explored with a TPR study. Fig. 5a compares the TPR profiles of calcined samples, C0.5Pt/NaM, C5Pt/NaM, and C5Pt/HM, with profiles of blank NaM and HM. In the profile of NaM, two large peaks in a wide range of temperatures, i.e., 183–220 and 220–340 K, are observed along with six minor sharp peaks in both positive and negative directions. Recently [23], these large and minor peaks have been assigned for a replacement of nitrogen by hydrogen and molecular chemisorption of nitrogen on sodium–oxygen ionic pairs at different locations in NaM, respectively.

In addition to the peaks described above, profiles of Pt/NaM samples in Fig. 5a also displayed two distinct peaks at ~ 300 and ~ 360 K. These two peaks are assigned to reduction of PtO_x in different locations, i.e., Pt_eO on the external surface (~ 300 K) and Pt_cO in the channel (~ 360 K), in accordance with the literature [3–13] on similar Pt-loaded samples of KL, (Na, K)-beta, NaY, silica, and alumina (see Table 1).

Fig. 5b presents the TPR profiles of recalcined samples. In addition to peaks observed with calcined samples, these recalcined samples showed a peak at $T_{\mathrm{r}} \sim 390$ K. This peak, in accordance with the literature [3–13], is assigned for the

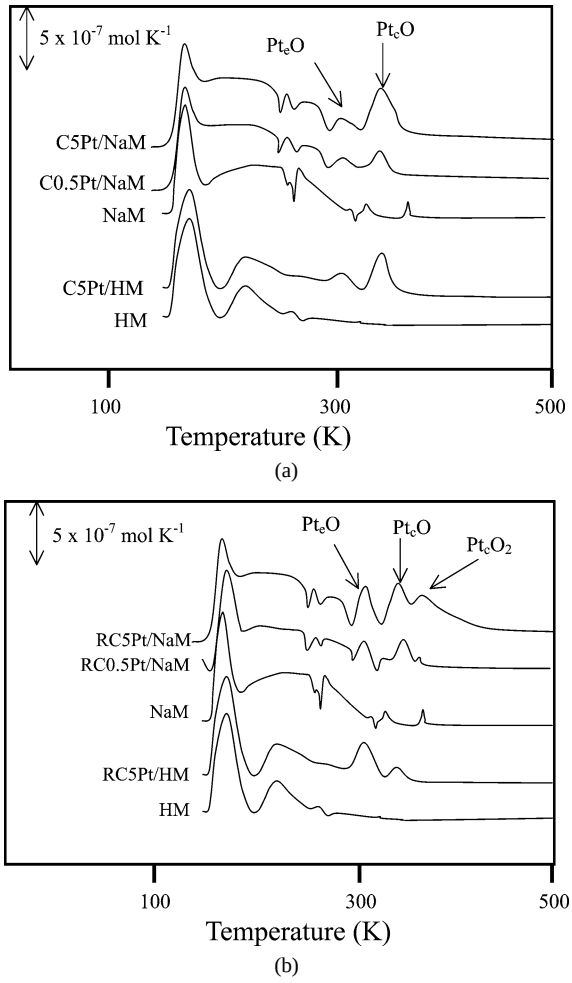

Fig. 5. Temperature-programmed reduction profiles of Pt samples (a) calcined and (b) recalcined.

reduction of Pt_cO_2 in the channel. Noticeably, a considerable enlargement of the peak at ~ 300 K in the profiles of recalcined samples confirmed the segregation of platinum particles from the channels of Pt/NaM and Pt/HM. The segregation during reduction is severe in RC5Pt/HM, whose TPR profile indicated that only a small fraction of platinum remained in channels.

Fig. 6 compares xenon uptake (N_{Xe}) isotherms, obtained at 296 K, of blank samples, HM and NaM, with reduced platinum samples. Observed uptakes in blank samples should have come from physisorption of xenon. In general, NaM exhibited a higher uptake at all xenon pressures than HM. Table 4 reveals that the xenon uptake on NaM at ~ 500 Torr ($N_{Xe} \sim 10.8 \times 10^{20}$ atoms g^{-1}) is about twice that ($N_{Xe} \sim 5.3 \times 10^{20}$ atoms g^{-1}) of HM (with a similar Si/Al ~ 10). Conceivably, xenon physisorption on the sodium ion in NaM is greater than the proton in HM.

A higher xenon uptake is generally observed in Fig. 6 for reduced Pt samples of Pt/NaM and Pt/HM than their blank mordenites. A small (0.5%) addition of platinum in both MOR samples increased the uptake. However, that the xenon uptake considerably decreased on R5Pt/NaM indicates a strong pore blockage probably by a large fraction of platinum remaining in the channels. This is in good agreement with the present hydrogen chemisorption results.

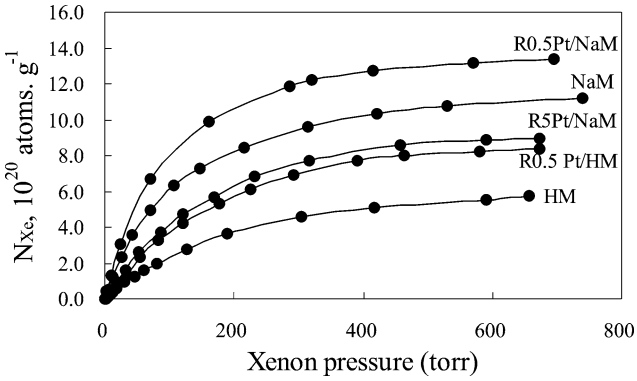

Fig. 6. Xenon adsorption isotherms measured at 296 K for calcined (C) and reduced (R) samples of Pt/NaM and Pt/HM along with blank samples of NaM and HM.

Table 4
Data obtained from xenon physisorption and ^{129}Xe NMR studies for blank NaM and HM and their Pt-loaded samples

Sample	N_{Xe} 10^{20} atoms g^{-1} (~ 500 Torr)	δ_c (ppm) (~ 500 Torr)	δ_0 (ppm)	Slope (ppm/ 10^{20} atoms g^{-1})	Channel volume = slope^{-1}, (10^{20} atoms g/ ppm)
NaM	10.8	138	84	4.91	0.20
R0.5Pt/NaM	13.0	151	88	4.93	0.20
R5Pt/NaM	8.7	162	101	6.95	0.14
HM	5.3	167[a]	–	–	–
R0.5Pt/HM	8.0	170[a]	–	–	–

[a] Shift for the coalesced peak.

In the literature, ^{129}Xe NMR spectra of NaM samples at 296 K displayed two broad peaks at chemical shifts of $\delta_p \sim 220$ and $\delta_c \sim 90$ ppm. They have been ascribed to xenon in the pocket (Xe_p) and in the channel (Xe_c) of mordenite structures, respectively [35–41]. The δ_c increases with P_{Xe} because of increasing Xe–Xe interactions. However, P_{Xe} virtually does not affect δ_p since the pocket ($d \sim 0.48$ nm) can accommodate only a single xenon ($d \sim 0.44$ nm) atom [35–37,40,41]

The similar two-peak pattern of ^{129}Xe NMR spectra of NaM is also observed for R0.5Pt/NaM samples at 296 K and is shown in Fig. 7. In order to know the effect of platinum in channels, the experimental δ_c values from R0.5Pt/NaM (Fig. 7) and R5Pt/NaM are plotted in Fig. 8 along with the δ_c values of NaM against N_{Xe} at various P_{Xe} noted from Fig. 6. The plots showed a linear increase in δ_c with N_{Xe} and the slope of the plots also increases with the Pt loading on MOR.

In Fig. 8, δ at $N_{Xe} \to 0$, i.e., δ_0, is given by the intercept of the plots drawn between δ_c and N_{Xe}. The δ_0 values for NaM, R0.5Pt/NaM, and R5Pt/NaM (84, 88, and 101 ppm, respectively) generally increased with their platinum loading. Since δ_0 is a reflection of the chemical environment

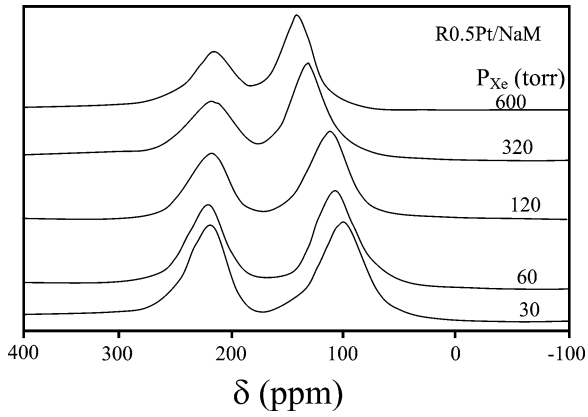

Fig. 7. ^{129}Xe NMR profiles of R0.5Pt/NaM recorded at 296 K with various P_{Xe}.

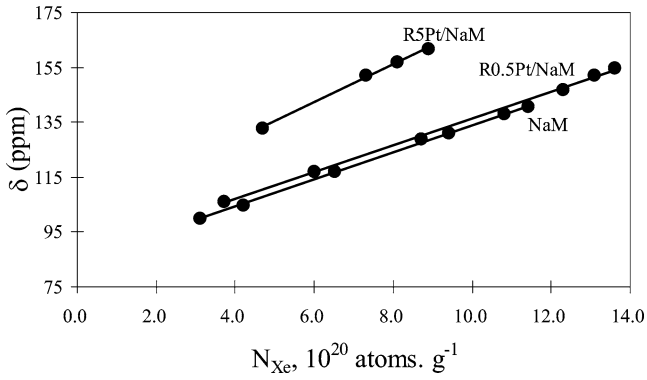

Fig. 8. A linear plot between the amount of xenon physisorbed per gram of a sample (N_{Xe}) and the chemical shift of xenon in channels.

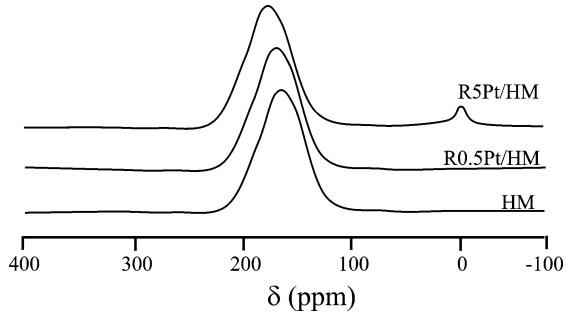

Fig. 9. ^{129}Xe NMR profiles of HM, R0.5Pt/HM, and R5Pt/HM at 296 K with $P_{Xe} \sim 500$ Torr.

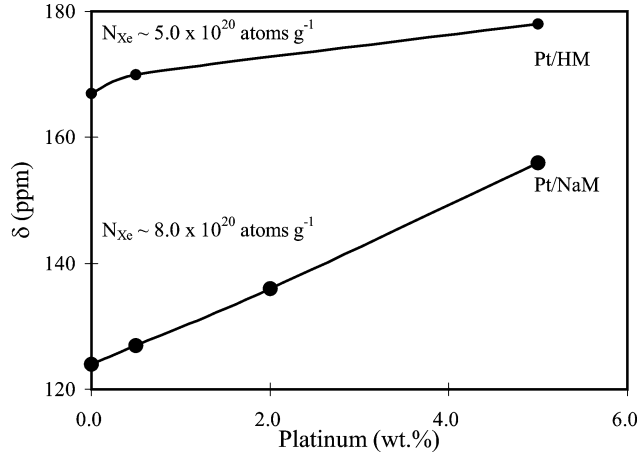

Fig. 10. Variation of chemical shift is plotted against the amount of platinum in a sample at a constant xenon loading.

of the channel surface, the density of platinum particles in the channel of R0.5Pt/NaM is insufficient to bring about a change in polarity of the channel surface in NaM. Consequently, the δ_0 value of the R0.5Pt/NaM sample had a negligible variation with that of NaM. On the other hand, the density of platinum deposited in the channels of R5Pt/NaM is high and enough to cause a significant increase to δ_0 of R5Pt/NaM sample.

Slopes for the plots of NaM, R0.5Pt/NaM, and R5Pt/NaM are noted as 4.91, 4.93, and 6.95 ppm/10^{20} atoms g^{-1}, respectively. The slope has been linearly related to local xenon density or, in other words, has been inversely related to channel volume [42]. From the slope values, channel volume (see column 6 of Table 4) of NaM (0.20×10^{20} atoms g ppm^{-1}) has not been altered by a tiny addition of platinum (as in R0.5Pt/NaM) but considerably decreased for R5Pt/NaM (0.14×10^{20} atoms g ppm^{-1}). The decrease is a resultant of a large quantity of platinum retained in channels during reduction and might block the diffusion of gases through pores. The pore blockage has also been envisaged from high δ_0 value for R5Pt/NaM sample and these ^{129}Xe NMR results are also in good agreement with the results of hydrogen chemisorption, xenon physisorption, TEM, and TPR studies.

Fig. 9 displayed a single peak in all three ^{129}Xe NMR profiles of HM, R0.5Pt/HM, and R5Pt/HM samples at 298 K with $P_{Xe} \sim 500$ Torr. It has been established that the δ_c and the δ_p in the profile of NaM coalesced to a single peak in the profile of HM sample [35,38] due to fast exchange of Xe_c with Xe_p. The peak at $\delta \sim 167$ ppm in blank HM is only slightly shifted to downfield in Pt samples, indicating a tiny amount of platinum remaining in the channel. In addition to the coalesced peak at $\delta \sim 178$ ppm for R5Pt/HM, a minor peak is also noted at $\delta \sim 0$ ppm. The appearance of the latter peak is probably due to an enhanced sensitivity toward bulk gaseous xenon in the presence of lot of metal particles at the external surface.

The δ_c of Pt/NaM and the single coalesced peak of Pt/HM, from their ^{129}Xe NMR spectra, are plotted in Fig. 10 against the platinum loading at $N_{Xe} \sim 8.0 \times 10^{20}$ and 5.0×10^{20} atoms g^{-1}, respectively. The linear increase of δ_c with the Pt content of the sample suggests that the fraction of platinum in channels of reduced Pt/NaM remained constant. Although the fraction is constant, large numbers of Pt particles in 5Pt/NaM should block the access of both hydrogen molecules and xenon, and the blockage eventually led to their low uptakes in isotherm measurements. This agrees well with the literature data on Pt/KL samples [22]. On the other hand, only a minor shift of the coalesced peak in Pt/HM to downfield suggested an extensive segregation of platinum from the channels during reduction treatment. Evidently, protons

in HM are ineffective in retarding the segregation of reduced platinum.

4. Conclusions

The present work on the segregation of platinum dispersed in Pt/MOR led to the following conclusions:

1. Pt particles were finely distributed on the fresh samples of ion-exchanged Pt/NaM and Pt/HM. Particles dispersed in channels segregated, mildly upon calcination but severely upon reduction, to the external surface of MOR.
2. The segregation was retarded by sodium ions in samples of Pt/NaM, which generally has a higher N_H/N_{Pt} ratio than Pt/HM.
3. Reduced platinum particles in different locations, i.e., in channel and on external surface of Pt/NaM, were characterized from their T_r temperature in TPR.
4. The platinum loading in Pt/NaM caused a linear downfield shift to the ^{129}Xe NMR peak characteristic to xenon in the channels. The linear shift suggested that the fraction of the Pt segregation was almost independent of the Pt loading.
5. Platinum aggregated at pore mouths of channels of reduced 5Pt/NaM substantially blocked diffusion of hydrogen and xenon into pores.

Acknowledgments

The authors thank the National Science Council for financial assistance and for a postdoctoral fellowship to one of the authors, S. Yuvaraj.

References

[1] R.J. Davis, Heterogeneous Chem. Rev. 1 (1994) 41.
[2] P. Meriadeau, C. Naccache, Catal. Rev. Sci. Eng. 39 (1997) 5.
[3] G. Moretti, W.M.H. Sachtler, J. Catal. 116 (1989) 350.
[4] J. Zheng, J.L. Dong, Q.H. Xu, Stud. Surf. Sci. Catal. 84 (1994) 1641.
[5] F.J.M. Hodar, M.F. Ribeiro, J.M. Silva, A.P. Antunes, F.R. Ribeiro, J. Catal. 178 (1998) 1.
[6] L.B. Gutierrez, A.V. Boix, E.A. Lombardo, J.L.G. Fierro, J. Catal. 199 (2001) 60.
[7] L.B. Gutierrez, A.V. Boix, J.O. Petunchi, J. Catal. 179 (1998) 179.
[8] L.W. Ho, C.P. Hwang, J.F. Lee, I. Wang, C.T. Yeh, J. Mol. Catal. A 136 (1998) 293.
[9] S.H. Park, M.S. Tzou, W.M.H. Sachtler, Appl. Catal. 24 (1986) 85.
[10] K. Foger, H. Jaeger, Appl. Catal. 56 (1989) 137.
[11] D.J. Ostgard, L. Kustov, K.R. Poeppelmeier, W.M.H. Sachtler, J. Catal. 133 (1992) 342.
[12] C.P. Hwang, C.T. Yeh, J. Catal. 182 (1999) 48.
[13] C.P. Hwang, C.T. Yeh, J. Mol. Catal. 112 (1996) 295.
[14] M. Boudart, L.C. de Menorval, J. Fraissard, G.P. Valenca, J. Phys. Chem. 92 (1988) 4033.
[15] G.P. Valenca, M. Boudart, J. Catal. 128 (1991) 447.
[16] R. Ryoo, C.H. Ko, J.M. Kim, R. Howe, Catal. Lett. 37 (1996) 29.
[17] R. Ryoo, S.J. Cho, C. Pak, J.G. Kim, S.K. Ihm, J.Y. Lee, J. Am. Chem. Soc. 114 (1992) 76.
[18] O.B. Yang, S.I. Woo, R. Ryoo, J. Catal. 123 (1990) 375.
[19] H. Ihee, T. Becue, R. Ryoo, C. Potvin, J.M. Monoli, G.D. Mariadassou, Stud. Surf. Sci. Catal. 84 (1994) 765.
[20] J. Zheng, J. Dong, Q. Xu, C. Hu, Catal. Lett. 37 (1996) 25.
[21] M. Sugimoto, H. Katsuno, T. Hayasaka, K.I. Hirasawa, N. Ishikawa, Appl. Catal. A 106 (1993) 9.
[22] S.J. Cho, W.S. Ahn, S.B. Hong, R. Ryoo, J. Phys. Chem. 100 (1996) 4996.
[23] S. Yuvaraj, T.H. Chang, C.T. Yeh, J. Phys. Chem. B 107 (2003) 4971.
[24] D. Exner, N. Jaeger, K. Moller, E.G. Schulz, J. Chem. Soc., Faraday Trans. 78 (1982) 3537.
[25] A.C.M. Van den Broek, J.V. Grondelle, R.A. Van Santen, Catal. Lett. 55 (1998) 79.
[26] W.M.H. Sachtler, Catal. Today 15 (1992) 419.
[27] R.E. Jentoft, M. Tsapatsis, M.E. Davis, B.C. Gates, J. Catal. 179 (1998) 565.
[28] J.T. Miller, N.G. Agarwal, G.S. Lane, F.S. Modica, J. Catal. 163 (1996) 106.
[29] M. Tsapatsis, M. Lovallo, T. Okubo, M.E. Davis, M. Saddakata, Chem. Mater. 7 (1995) 1734.
[30] J.R. Anderson, in: Structure of Metallic Catalysts, Academic Press, New York, 1975, p. 365.
[31] S.C. Chou, C.T. Yeh, J. Chem. Soc., Faraday Trans. 92 (1996) 1409.
[32] S. Feast, M. Englisch, A. Jentys, J.A. Lercher, Appl. Catal. A 174 (1998) 155.
[33] N. Ichikuni, Y. Iwasawa, Catal. Lett. 20 (1993) 87.
[34] P. Gallezot, A.A. Diaz, J.A. Dalmon, A.J. Renouprez, B. Imelik, J. Catal. 39 (1975) 334.
[35] J.A. Ripmeester, J. Am. Chem. Soc. 104 (1982) 289.
[36] J.A. Ripmeester, J. Magn. Reson. 56 (1984) 247.
[37] J.A. Ripmeester, C.I. Ratcliff, J. Phys. Chem. 94 (1990) 7652.
[38] J.H. Yang, L.A. Clark, G.J. Ray, Y.J. Kim, H. Du, R.Q. Snurr, J. Phys. Chem. B 105 (2001) 4698.
[39] E.E. Miro, L. Costa, J.M. Dereppe, J.O. Petunchi, Stud. Surf. Sci. Catal. 111 (1997) 231.
[40] J. Nagano, T. Eguchi, T. Asanuma, H. Masui, H. Nakayama, N. Nakamura, E.G. Derouane, Micropor. Mesopor. Mater. 33 (1999) 249.
[41] M.A. Springuel-Huet, J.P. Fraissard, Zeolites 12 (1992) 841.
[42] J.L. Bonardet, J. Fraissard, A. Gedeon, M.A. Springuel-Huet, Catal. Rev. Sci. Eng. 41 (1999) 124.